The IAG/IAPSO Joint Working Group on Geodetic Effects of Nontidal Oceanic Processes

by

Richard S. Gross

Jet Propulsion Laboratory
California Institute of Technology
Pasadena, CA 91109–8099, USA

XXIII General Assembly of the IUGG

June 30, 2003 – July 11, 2003
Sapporo, Japan

- **The oceans have a major impact on global geophysical processes of the Earth**
  - Oceanic currents and bottom pressure
    - Affect the Earth's rotation (length-of-day, polar motion, nutation)
  - Redistribution of oceanic mass
    - Causes temporal variations of the Earth's gravitational field
    - Affects the Earth's geocenter (center-of-mass of solid Earth)
    - Loads the oceanic crust and mantle, thereby affecting the positions of stations located near the oceans
- **IAG/IAPSO Joint Working Group**
  - Formed in 1999 at XXII General Assembly of IUGG (Birmingham)
  - Promote investigations of the effects of nontidal oceanic processes on the Earth's rotation, deformation, gravitational field, and geocenter
  - Foster interactions between the geodetic and oceanographic communities in order to gain greater understanding of these effects

Bibliography (1999–2003)

Boussinesq Ocean Models & Mass Conservation	**6**
Oceanic Angular Momentum	**1**
and Length-of-Day	13
and Polar Motion	23
Oceanic Torques	**3**
and Polar Motion	1
Inverted Barometer Approximation	
Tide Gauge Data	5
Satellite Altimetry	6
Models	5
Theory	1
Ocean-Bottom Pressure	
Measurements	1
Models	3
Ocean Loading (Nontidal)	**2**
Gravitational Field Changes	**11**
Geocenter	**9**
Total	**90**

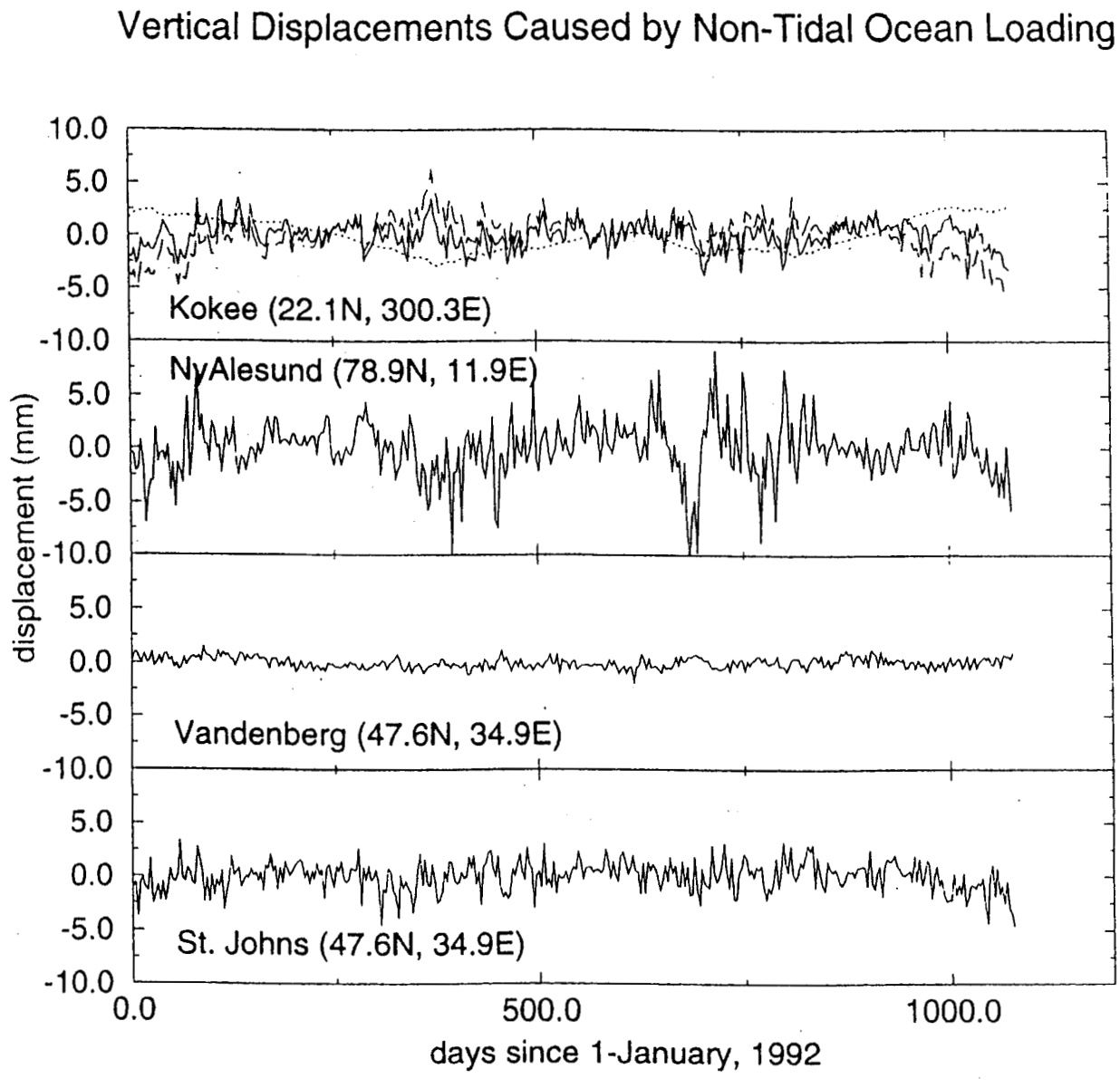

Figure 1. Vertical crustal motion at four coastal GPS sites, caused by non-tidal ocean loading and predicted by the OGCM model. The results are the sum of contributions from the sea-surface and density effects. Results for the sea-surface (dashed line) and density effect (dotted line) contributions are shown separately for Kokee.

© 1997 RAS, *GJI* 129, 507–517

vanDam et al. (1997)

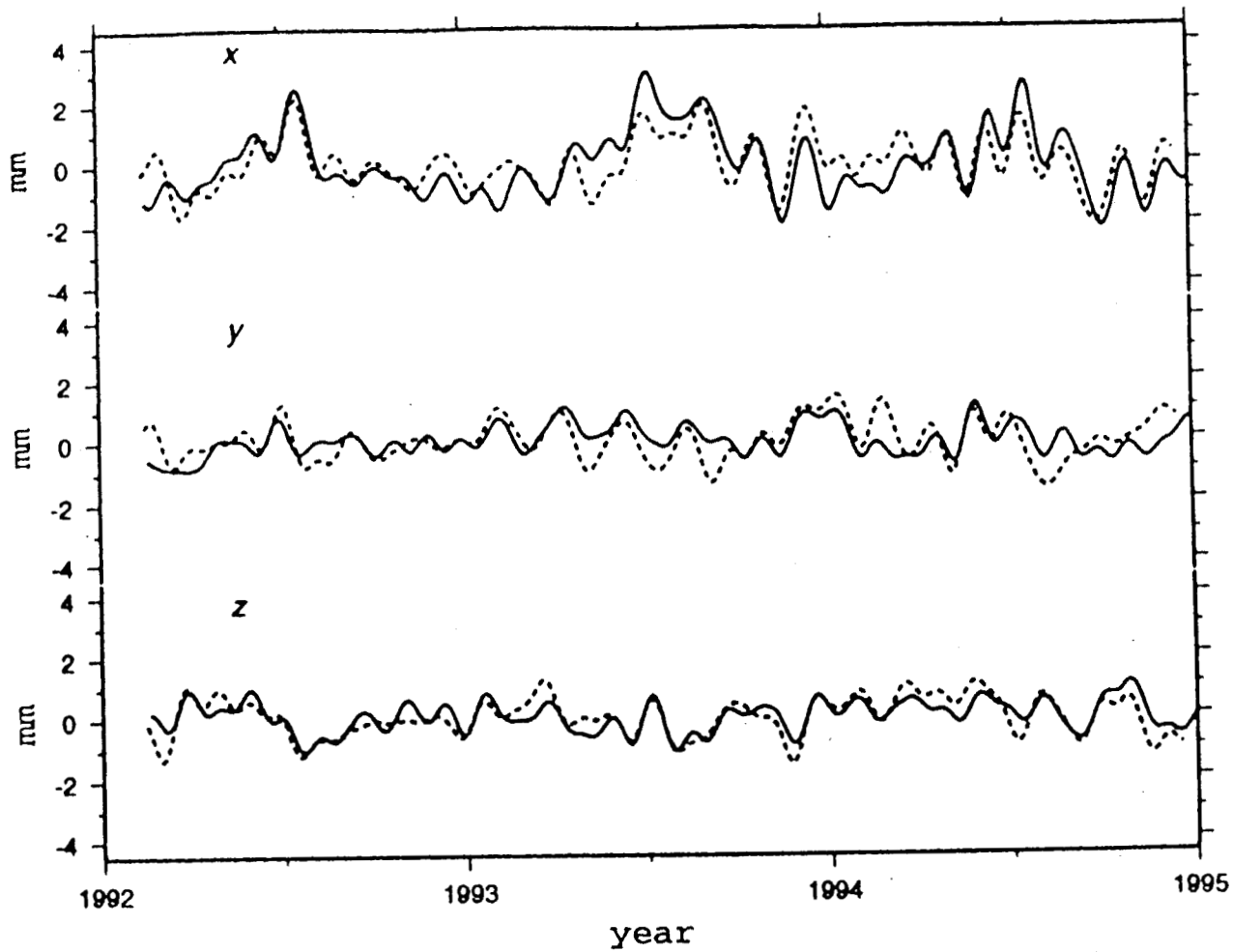

Figure 2: Geocenter variation from ISO model (solid line) and MOM model (dashed line). Both series passed band-pass filtering with the cutoff period from 30 day to 10 year.

Dong et al. (1997)

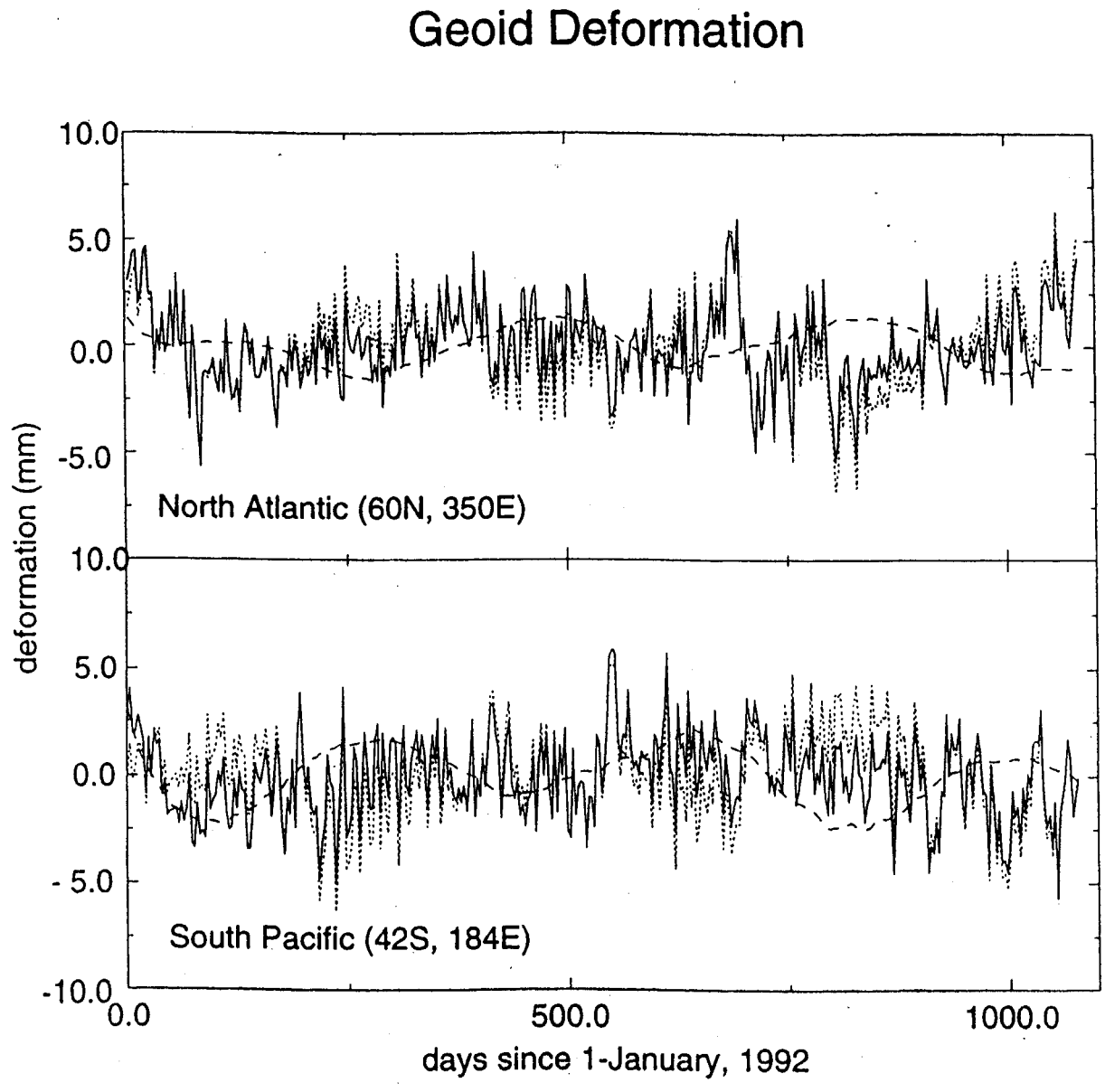

Figure 3. Time-dependent fluctuations in the geoid due to non-tidal ocean loading, estimated at two representative sites in the North Atlantic and South Pacific using results from the OGCM model. Results for the sea-level (dotted line) and density effect (dashed line) contributions and for the sum of the two (solid line) are shown for each location.

vanDam et al. (1997)

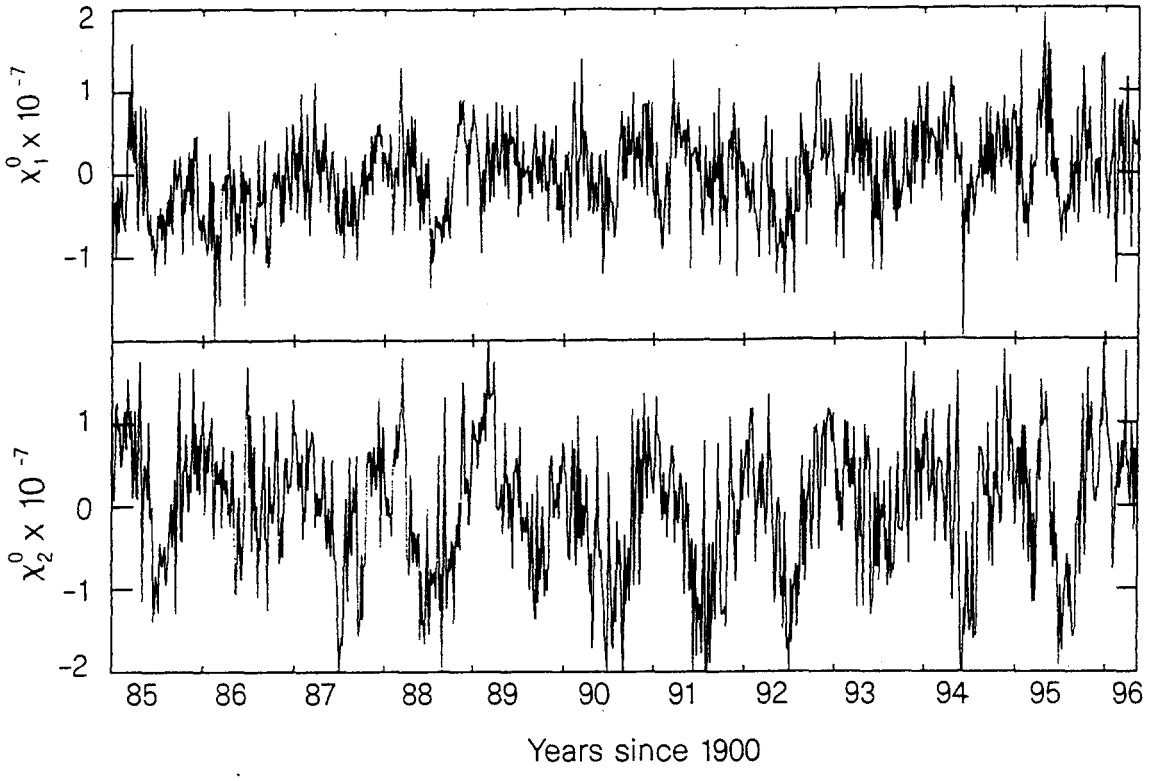

Figure 1 Five-day averaged values of χ_1^O and χ_2^O for the period January 85–April 96. Means have been removed. χ_1^O and χ_2^O are dimensionless and essentially proportional to the oceanic angular momentum about the two equatorial axes, conventionally taken to point towards the Greenwich and 90° E meridians, respectively[5]. The functions incorporate effects of the elasticity of the Earth and thus represent the effective excitation of polar motion by the oceans[1,5]. The time series show a rich variability over a wide range of timescales, and with no significant long term trends. The seasonal cycle is most conspicuous in χ_2^O, which tends to have slightly larger amplitudes than χ_1^O.

Ponte et al. (1998)

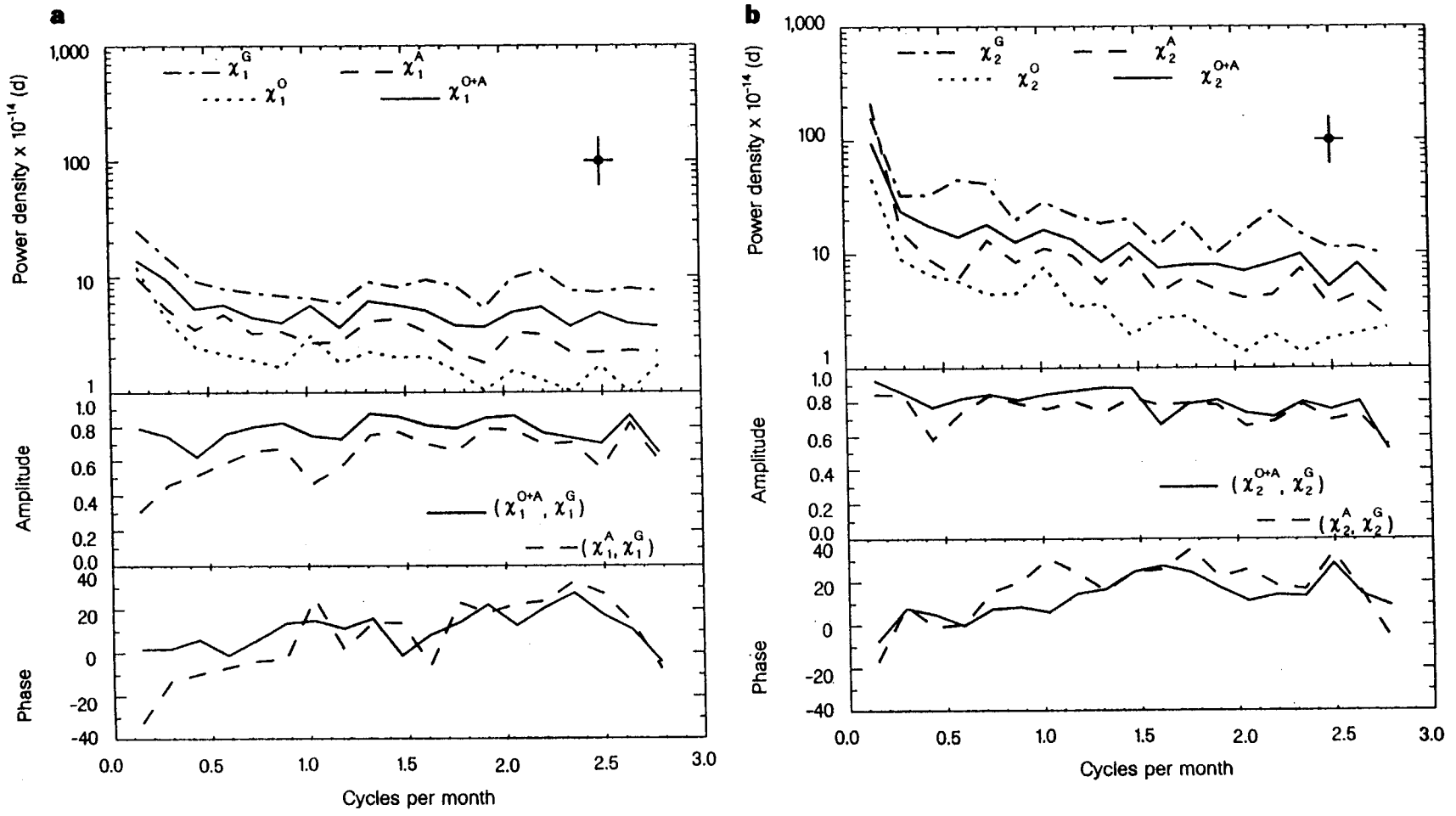

Figure 3 Assessment of oceanic effects on the excitation of polar motion. **a**, Power spectral density of χ_1^O, χ_1^A, χ_1^{O+A}, χ_1^G, and coherence amplitude and phase in degrees for the pairs (χ_1^A, χ_1^G) and (χ_1^{O+A}, χ_1^G). Similar curves for χ_2 series are shown in **b**. Power spectral density and coherence are calculated with band-averaging over 20 frequencies. 95% confidence limits for the spectra are shown on the upper right (vertical bar), together with the bandwidth (horizontal bar). Coherence amplitudes >0.38 are significantly different from zero at the 95% confidence level.

Ponte et al., (1998)

Atmospheric and Non-tidal ocean loading

- Radial atmospheric loading displacements computed globally from 9 years (1992-2000) of NCEP reanalysis daily mean pressure fields.
- Radial non-tidal ocean loading displacements computed globally from 5 years (1996-2000) of daily mean ocean bottom pressure fields derived from JPL OCM (Fukumori et al.).
  - OCM only includes wind forcing, and does not include pressure forcing.
  - Effects of non-IB response, and sub-daily variations not considered.
- Variance and maximum of each of these displacements mapped. (units are mm^2 and mm in maps)

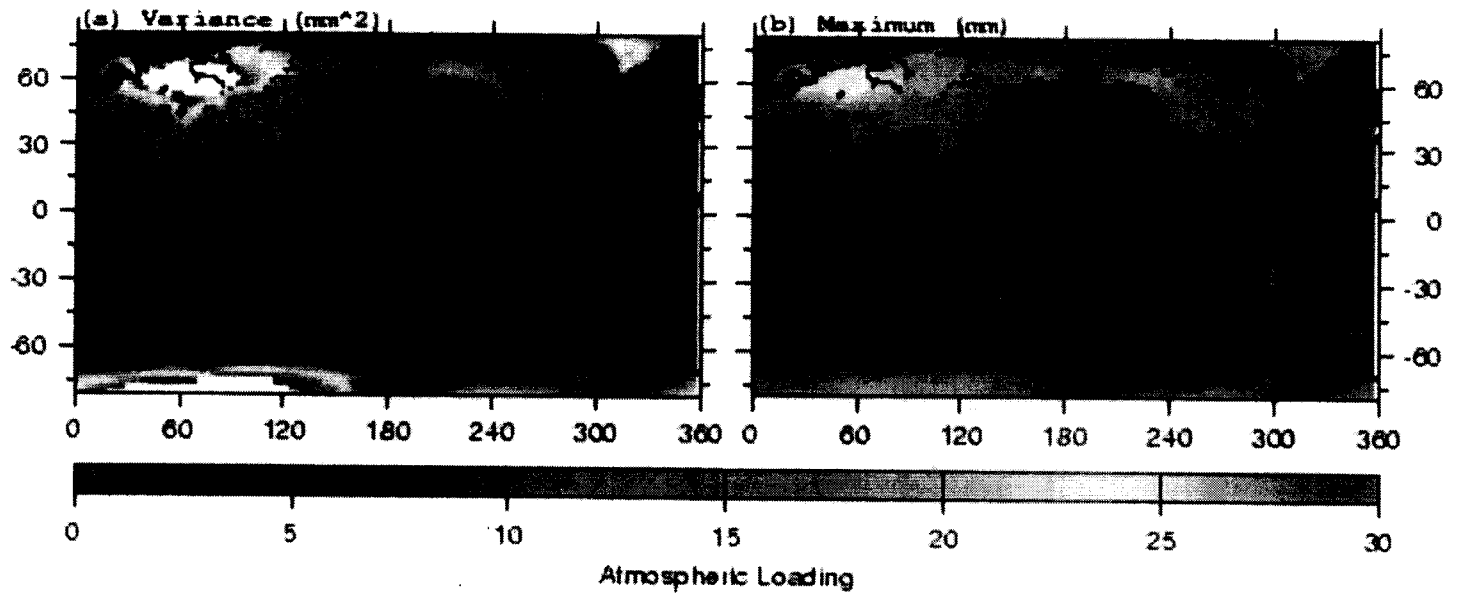

Atmospheric Loading

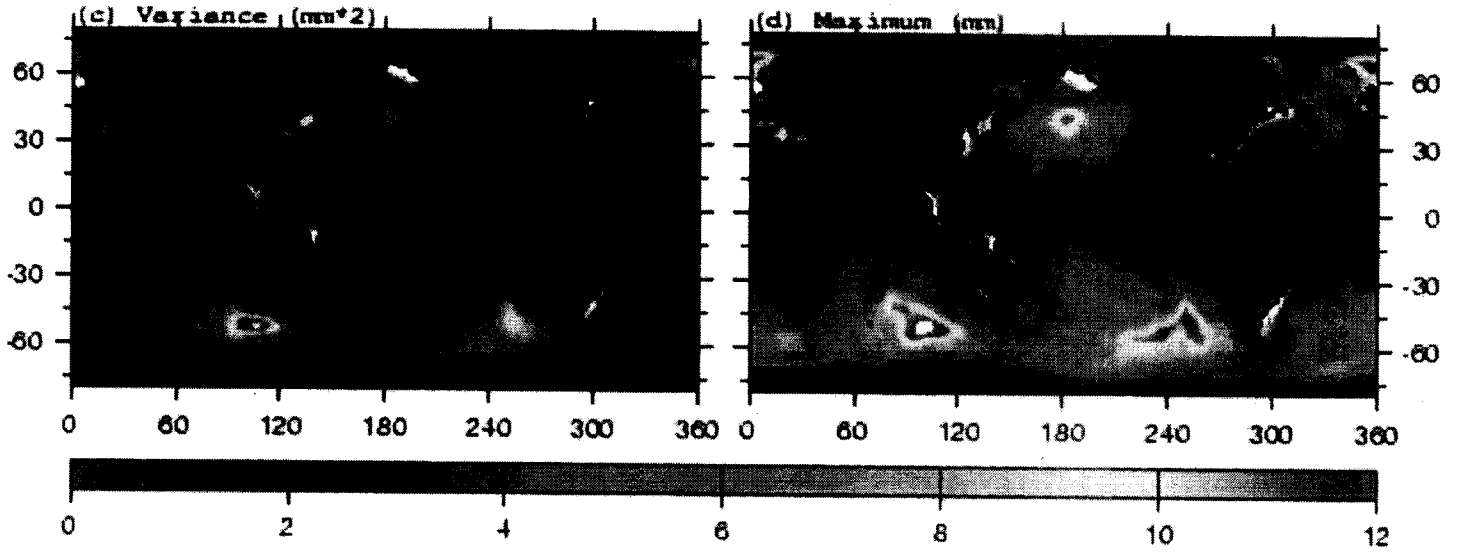

Non-tidal Ocean Loading

Variance Reduction of Radial GPS Site Displacements from Atmospheric Loading

- NCEP Reanalysis fields adopted
- Variance maps used to infer 100 available GPS sites with largest expected atmospheric loading variance
- Variance reduction at these sites shown below.
- Variance reduced at all but 10(5) sites when variance reduction computed w.r.t. linear (linear+annual+semiannual) functions.

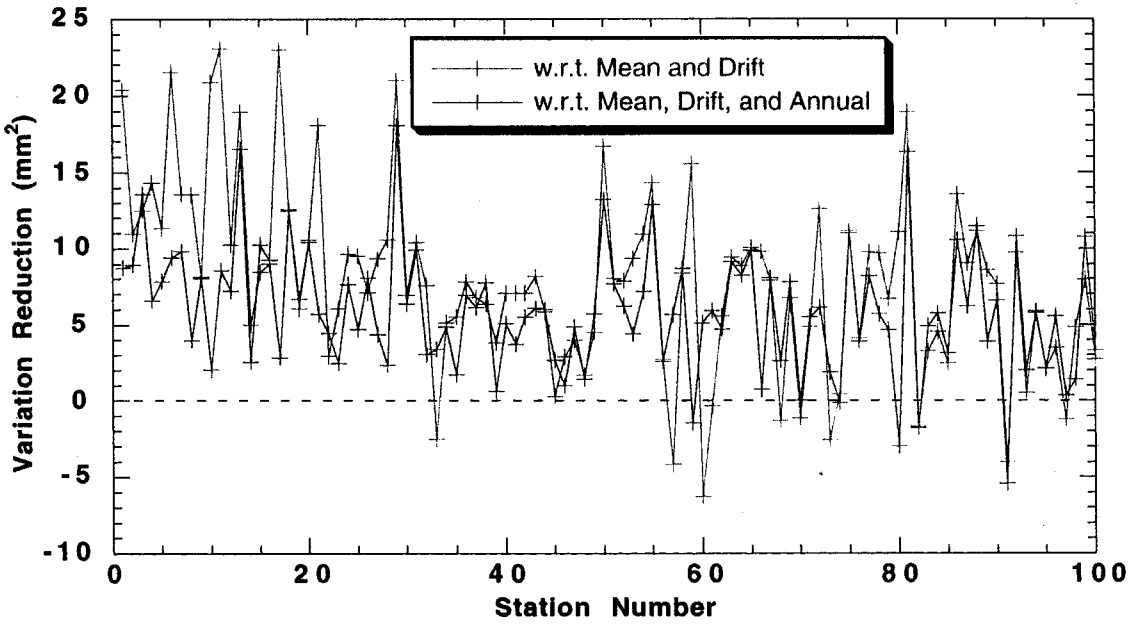

Variance Reduction of GPS Site Displacements from Non-tidal Ocean Loading

- Ocean bottom pressures from JPL OCM (Fukumori et al.) adopted
- Variance maps used to infer 23 available GPS sites with largest expected non-tidal ocean loading variance
- Variance reduction at these sites shown below.
- Variance reduced at 19(13) sites when variance reduction computed w.r.t. linear (linear+annual+semiannual) functions.

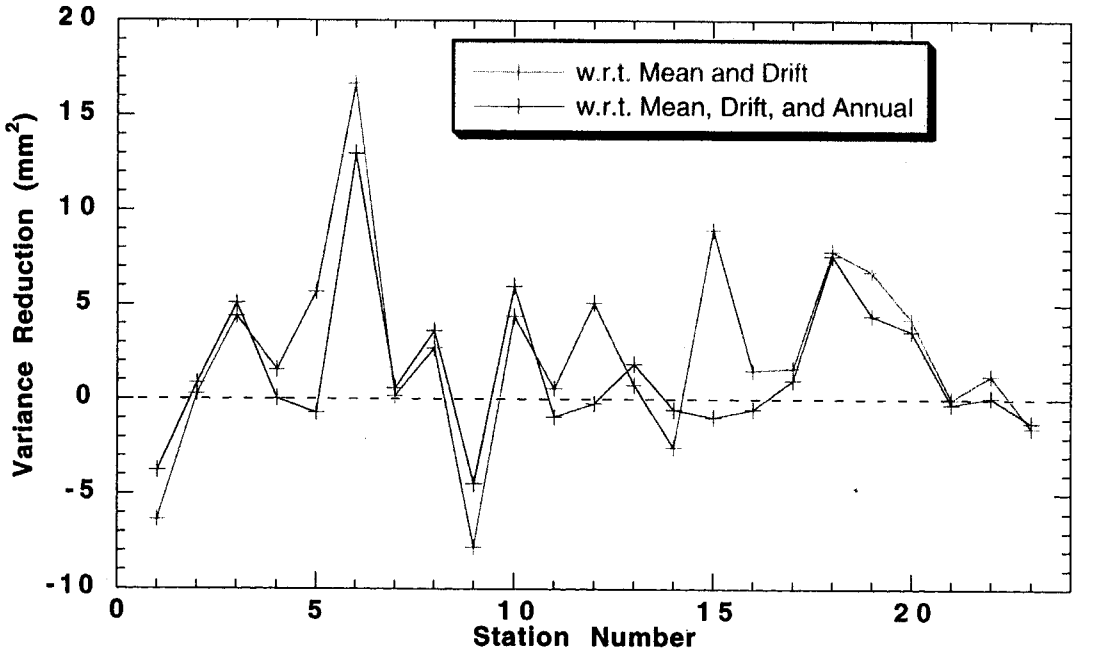

DATA SETS

- **Polar motion and length-of-day observations**
  - COMB2000 combined Earth orientation series
    - Kalman filter-based combination of optical astrometric, satellite and lunar laser ranging, very long baseline interferometry, and global positioning system measurements
    - Daily values at midnight spanning 1962–2000
  - Kalman filter self-consistently estimates polar motion rate and hence polar motion excitation function
- **Atmospheric angular momentum**
  - NCEP/NCAR reanalysis atmospheric angular momentum series
    - 6-hour values spanning 1958–present
    - Pressure term used is that computed assuming oceans respond as inverted barometer to imposed atmospheric pressure changes
  - Average over diurnal cycle by forming centered average of 5 successive values with weights 1/8, 1/4, 1/4, 1/4, 1/8
  - Convert to equivalent lod and polar motion excitation functions
- **Oceanic angular momentum**
  - Angular momentum due to current and ocean-bottom pressure fluctuations computed from MIT ocean model run at JPL (ECCO)
    - Daily values at midnight spanning 1980–2000
  - Convert to equivalent lod and polar motion excitation functions
  - Correct ocean-bottom pressure term for effects of mass non-conservation (Boussinesq ocean models conserve volume)

BOUSSINESQ MODELS

- The Boussinesq approximation is commonly used in ocean general circulation models (OGCMs)
  - Density variations in oceans are small
    - Usually less than ± 2.5% of average density
  - Under Boussinesq approximation, density variations are ignored except in the gravitational buoyancy force
    - Density is not constant but changes as temperature, pressure, and salinity changes
- Boussinesq models conserve volume, not mass
  - Under Boussinesq approximation, conservation of mass equation $\nabla \cdot (\rho \mathbf{u}) = 0$ reduces to $\nabla \cdot \mathbf{u} = 0$ (conservation of volume)
- In Boussinesq ocean models, imposed heat flux can lead to model mass changes
  - Imposed heat flux ⇒ temperature changes ⇒ density changes via equation of state
  - Since model volume is constant, model mass must change to accommodate density change
    - Boussinesq models do not properly represent steric sea level, but can be corrected to do so (e.g., Greatbatch, 1994; Mellor & Ezer, 1995)
- Must account for mass non-conservation
  - Add layer of fluctuating thickness to ocean surface
    - Compute effect of mass conserving layer on OAM, bottom pressure, etc.

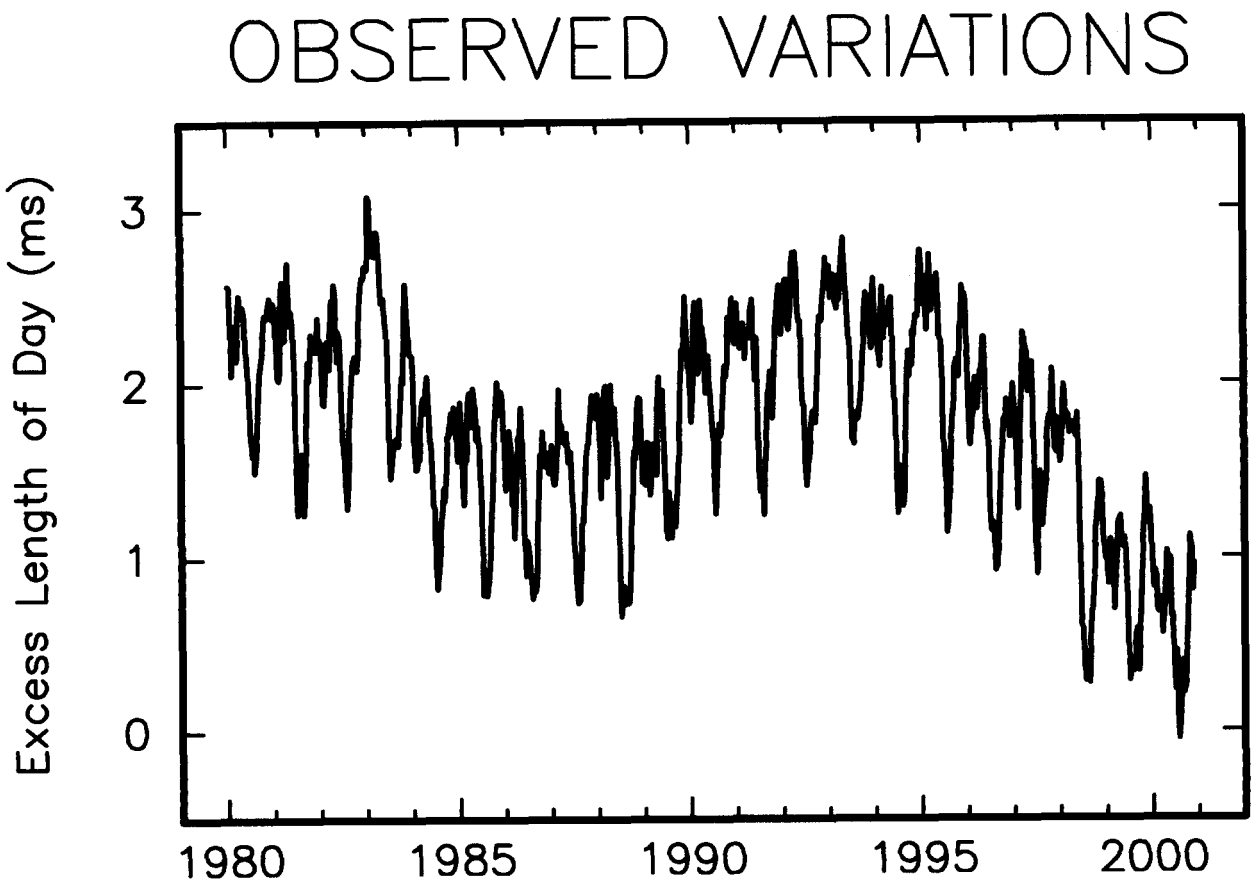

Figure 1. The COMB2000 series of observed length-of-day variations during 1980–2000 from which tidal effects have been removed. For purposes of clarity of display, 10-day averages of the observed daily values are shown.

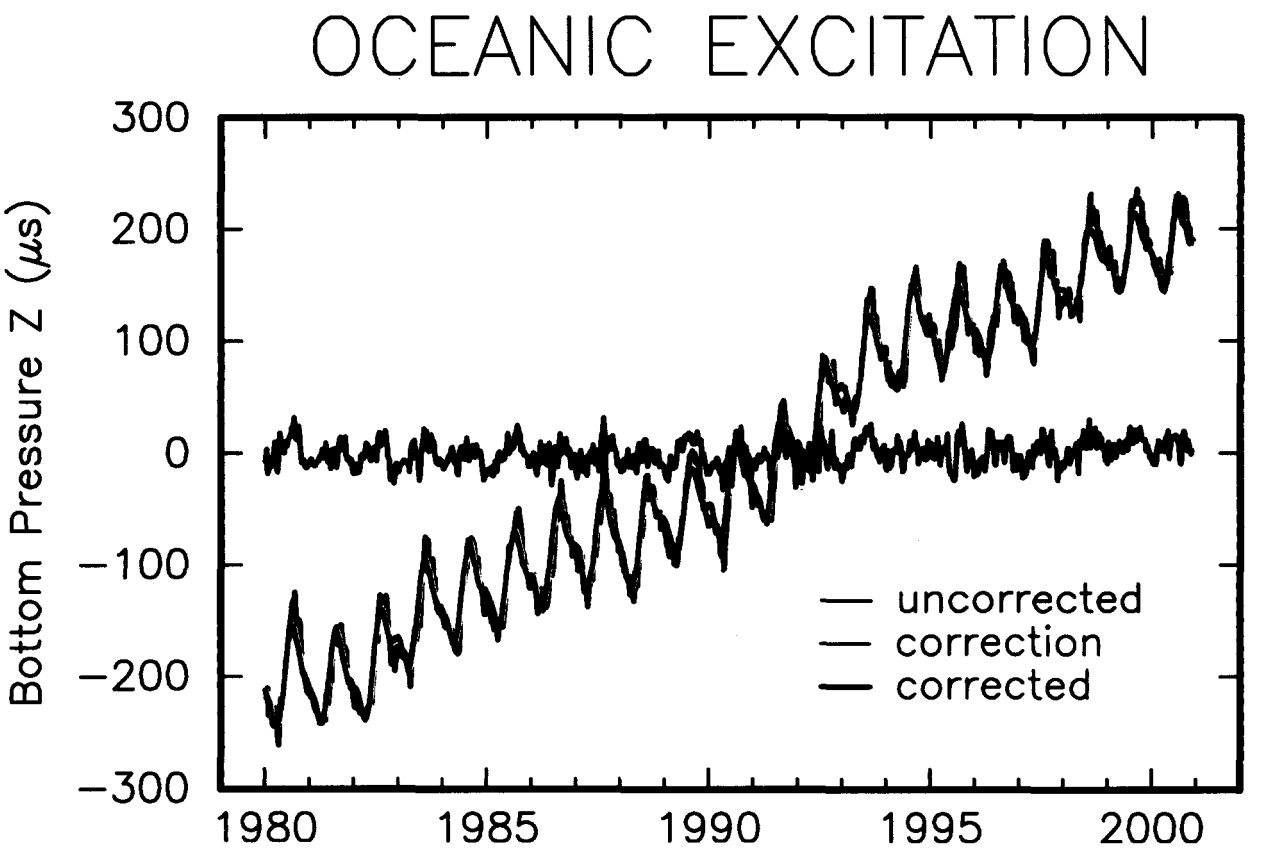

Figure 2. The axial component of the angular momentum associated with ocean-bottom pressure variations, in equivalent length-of-day units, both before (diagonal black curve) and after (horizontal blue curve) correcting it for the effects of artificial mass variations due to the use of the Boussinesq approximation in the MIT ocean model. The correction that has been applied to the pressure OAM term is shown by the smoother red curve overlying the uncorrected values shown in black. For purposes of clarity of display, 10-day averages of the hourly OAM values are shown.

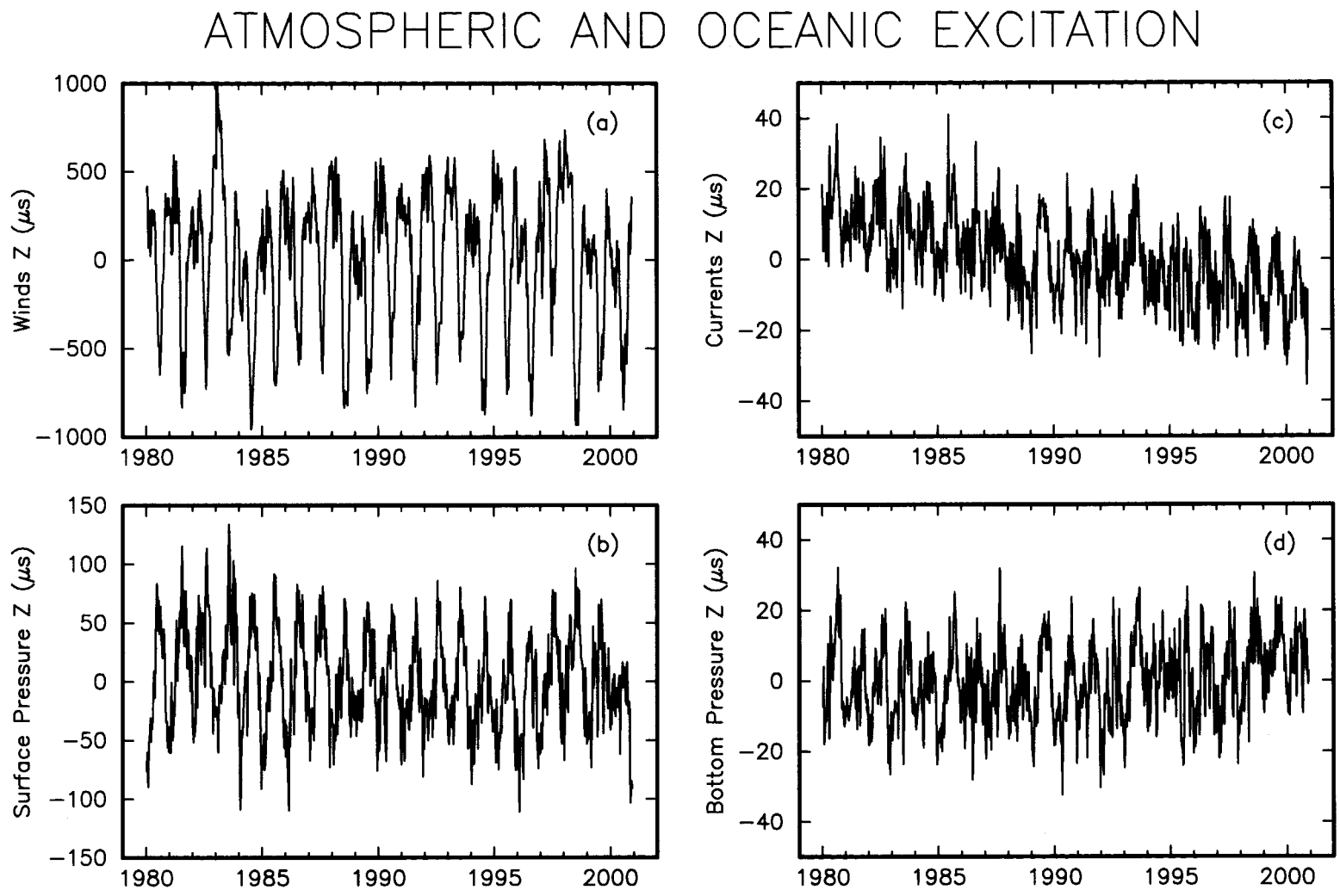

Figure 3. The z-component of the angular momentum, in equivalent length-of-day units, associated with: (a) atmospheric winds, (b) atmospheric surface pressure variations, (c) oceanic currents, and (d) ocean-bottom pressure variations. The angular momentum associated with atmospheric surface pressure variations has been computed assuming the oceans respond as an inverted barometer to the imposed surface pressure variations. For purposes of clarity of display, 10-day averages are shown.

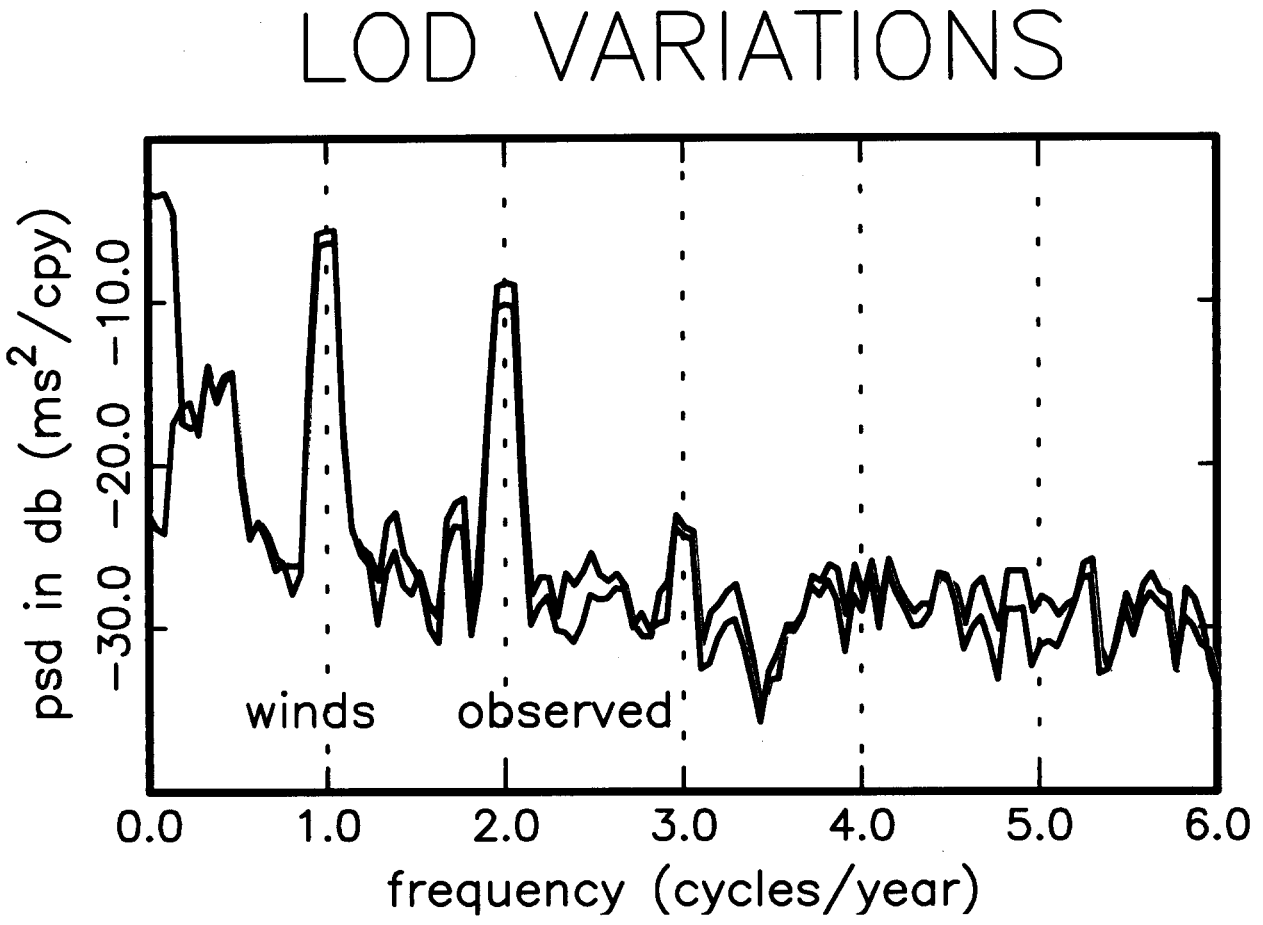

Figure 4. Power spectral density (psd) estimates in decibels (db) computed by the multitaper method from time series spanning 1980–2000 of: (a) the observed COMB2000 length-of-day variations derived from astrometric and space-geodetic Earth orientation measurements (black curve), (b) the LOD excitation due to atmospheric winds below 10 hPa (red curve).

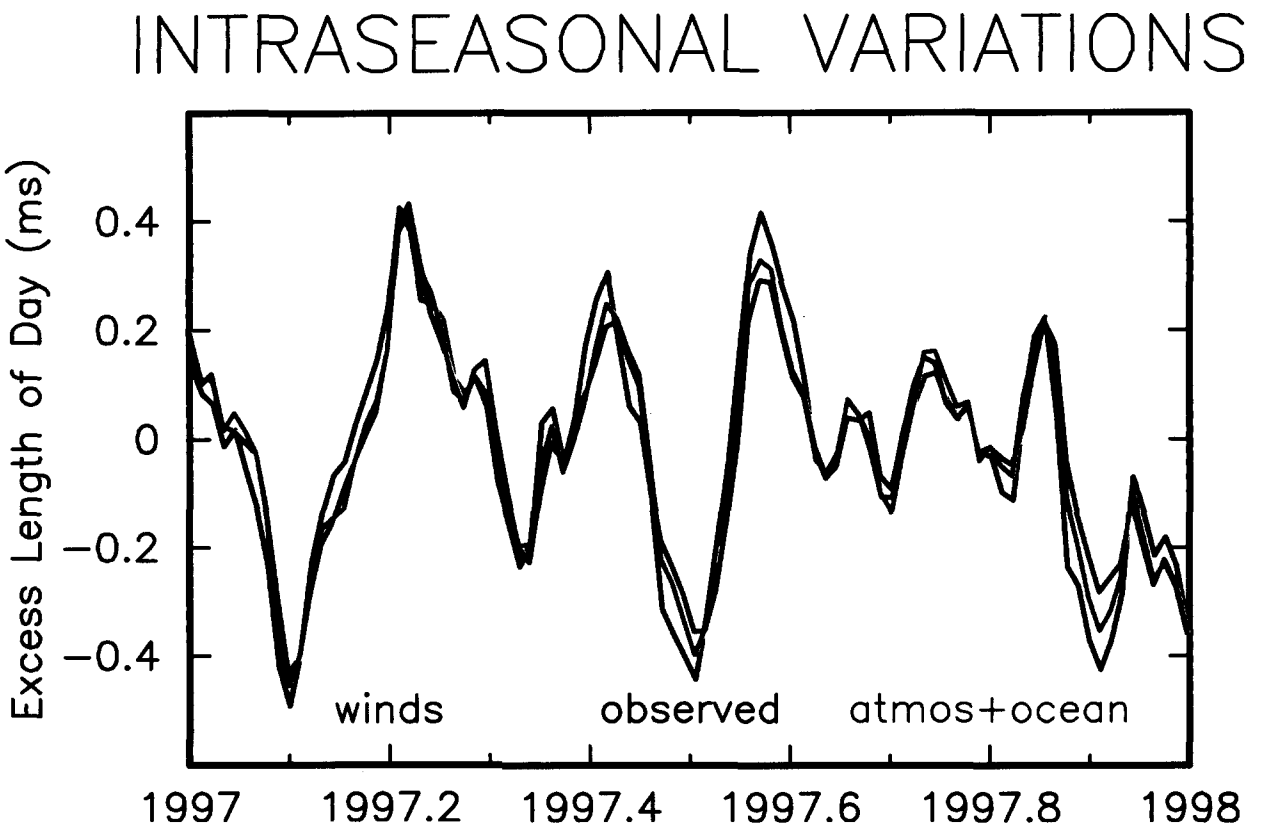

Figure 5. Observed length-of-day variations (black); variations caused by the modeled atmospheric winds (red); and variations caused by the sum of the modeled atmospheric winds, surface pressure, oceanic currents, and bottom pressure (blue) on intraseasonal time scales during 1997. Intraseasonal variations considered here have periods ranging between 4 days and 1 year excluding signals at the annual, semiannual, and terannual frequencies. The atmospheric surface pressure term is that computed assuming the oceans respond as an inverted barometer to the imposed surface pressure variations. The contribution to intraseasonal LOD variations of the winds between 10 hPa and 0.3 hPa is included in the red and blue curves.

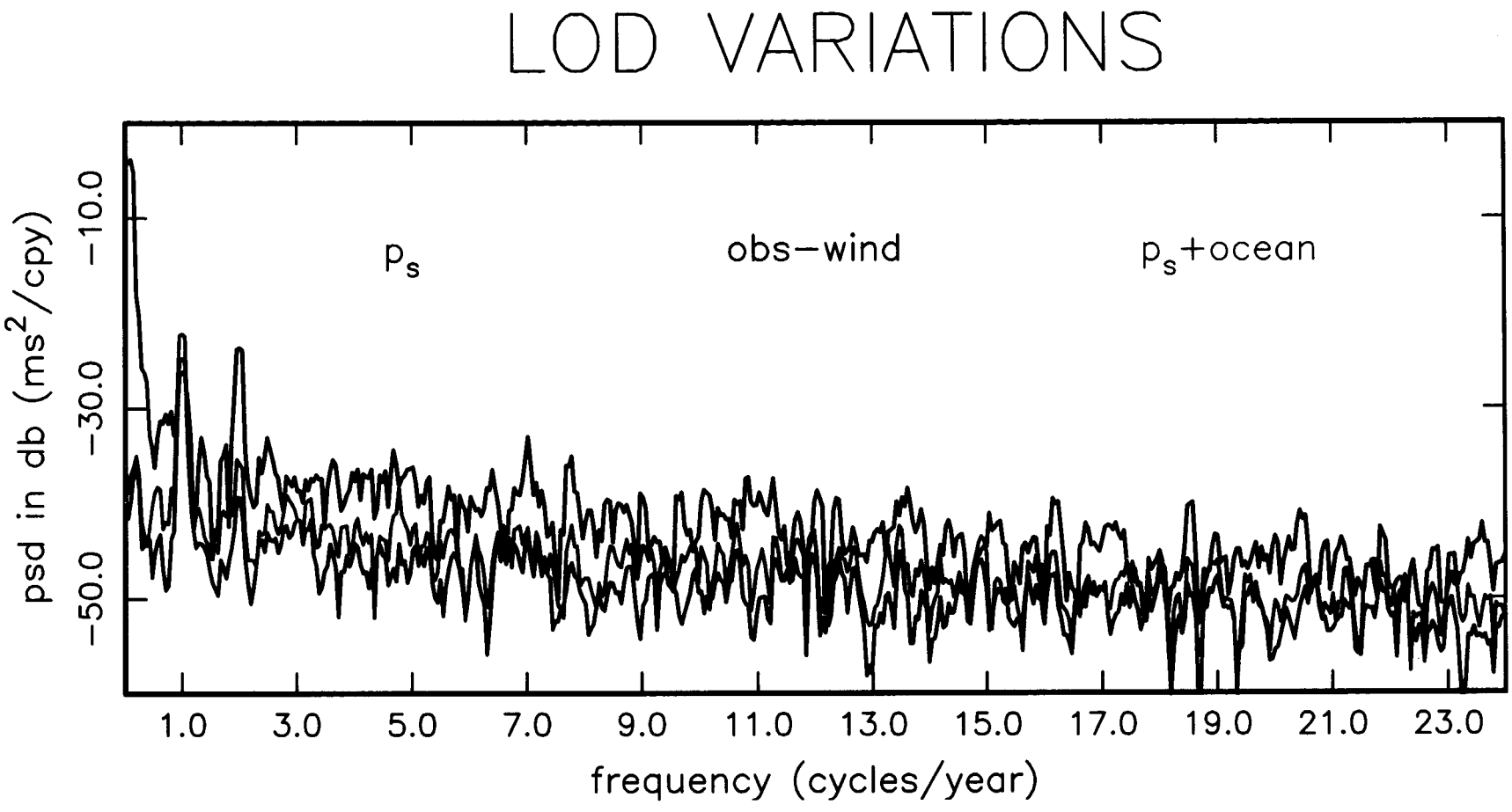

Figure 6. Power spectral density (psd) estimates in decibels (db) computed by the multitaper method from time series spanning 1980–2000 of: (a) the difference between the observed length-of-day variations and that caused by changes in the atmospheric winds (upper black curve), (b) LOD variations caused by atmospheric surface pressure p_S changes (lower red curve), and (c) LOD variations caused by the sum of atmospheric surface pressure, oceanic currents, and ocean-bottom pressure changes (middle blue curve). Variations at the annual, semiannual, and terannual frequencies were not removed from the data sets prior to spectral estimation.

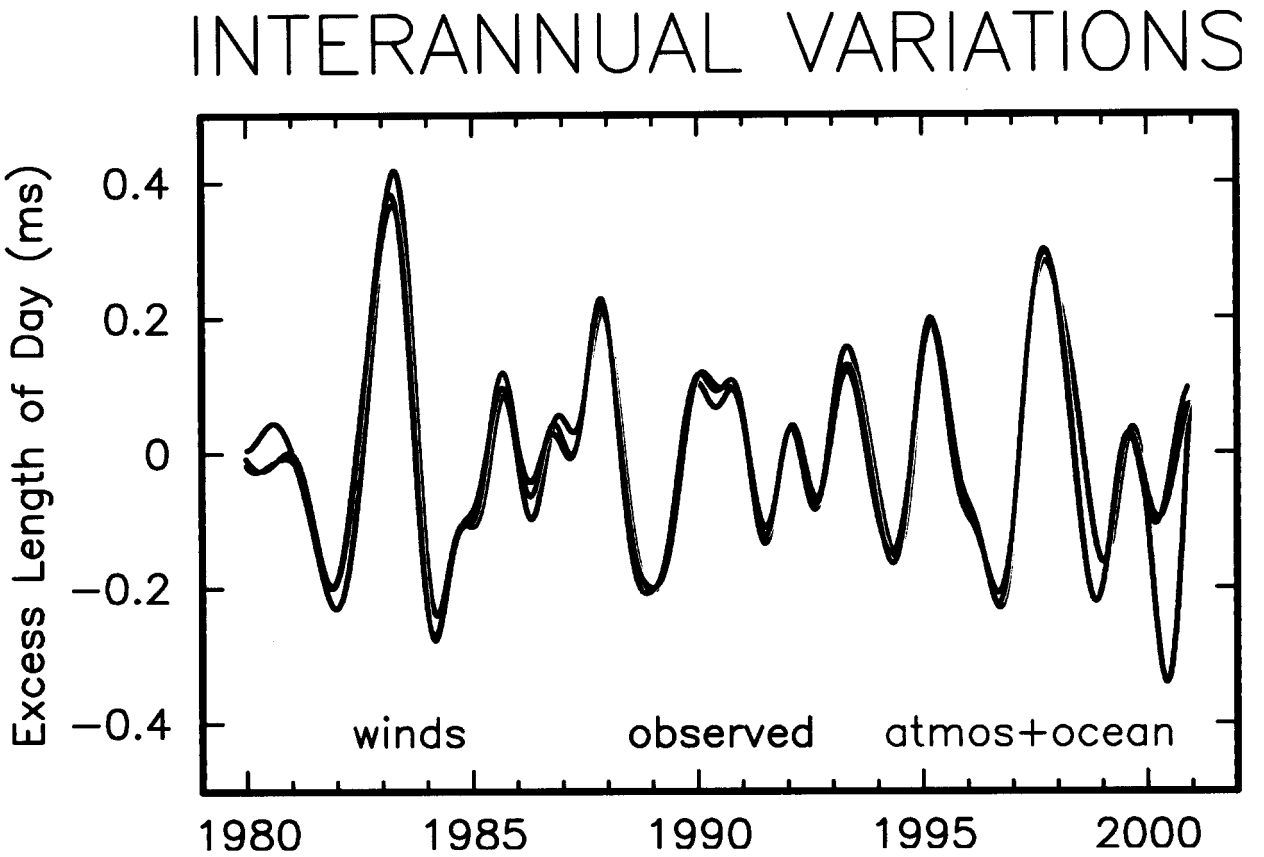

Figure 7. Observed length-of-day variations (black); variations caused by the modeled atmospheric winds (red); and variations caused by the sum of the modeled atmospheric winds, surface pressure, oceanic currents, and ocean-bottom pressure (blue) on interannual time scales during 1980–2000. The interannual frequency band ranges from 1/5 cpy to 1 cpy. The atmospheric surface pressure term is that computed assuming the oceans respond as an inverted barometer to the imposed surface pressure variations.

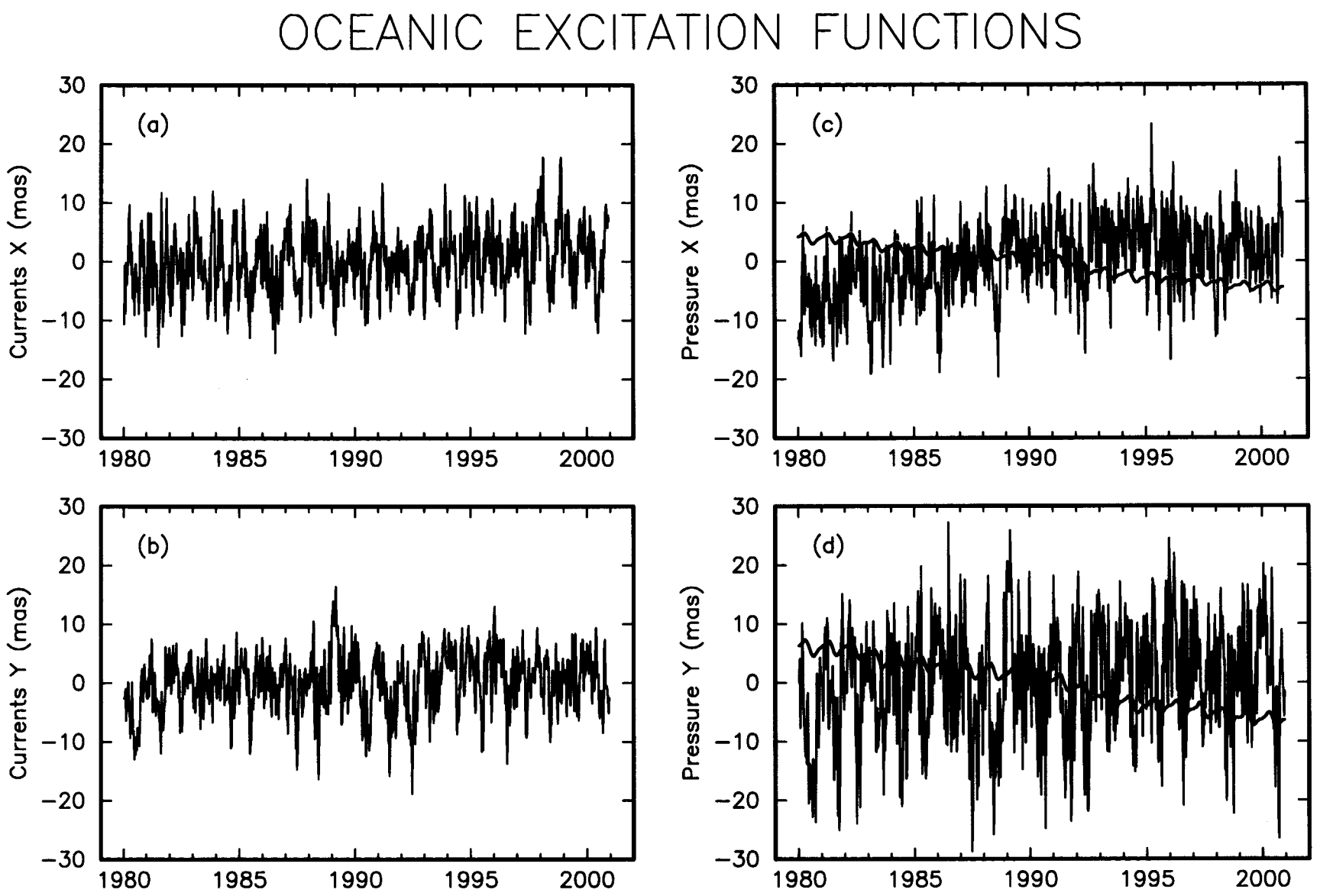

Figure 1. The *x*- and *y*- components of the oceanic excitation functions due to variations in oceanic currents (a and b, respectively) and ocean-bottom pressure (c and d, respectively). For purposes of clarity of display, 10-day averages of the daily oceanic excitation functions are shown. In (c and d), the red curves show the correction that was applied to the pressure term as a result of enforcing mass conservation. The black curves show the final pressure excitation functions after the correction was applied.

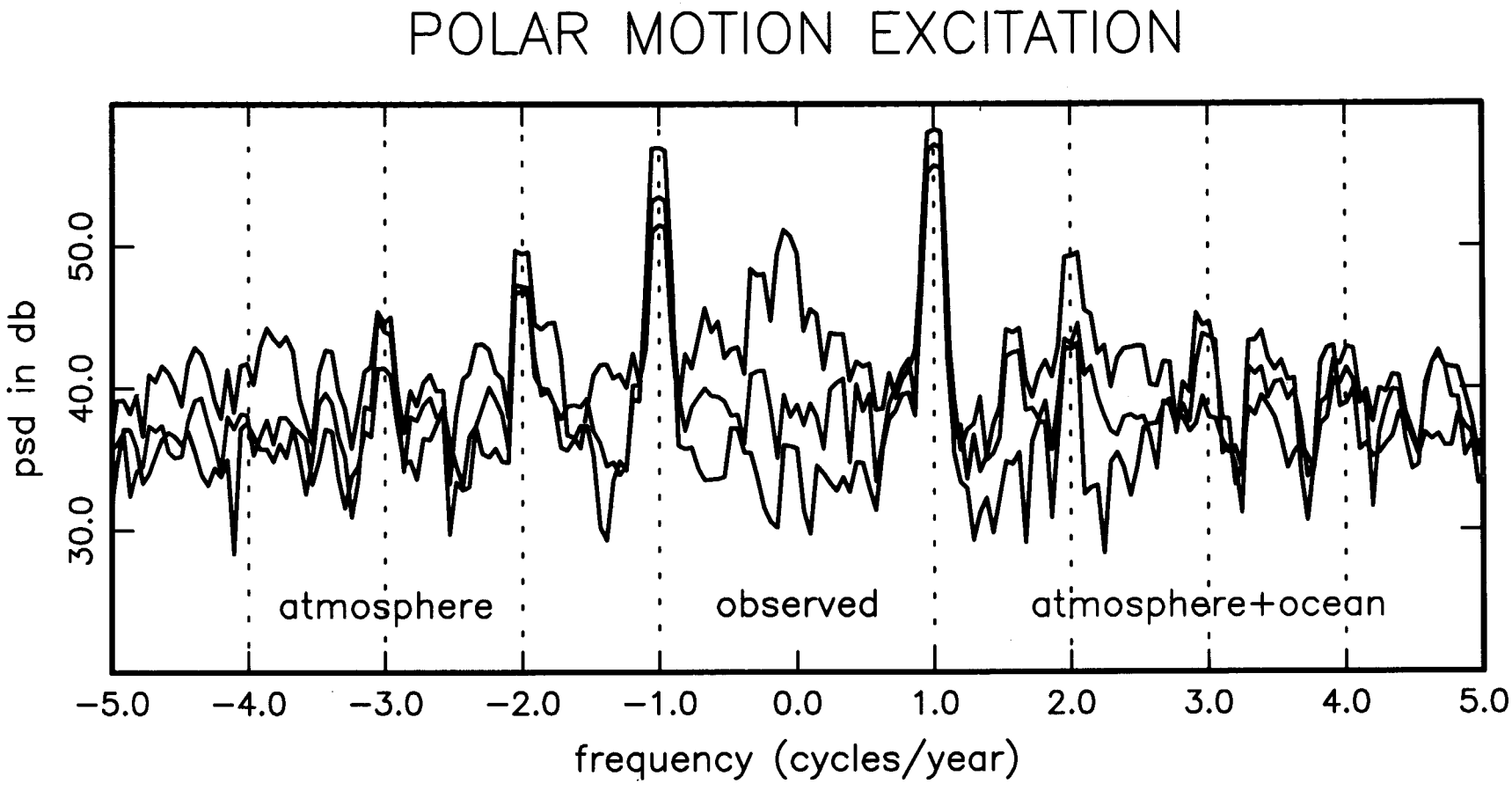

Figure 2. Power spectral density (psd) estimates in decibels (db) computed by the multitaper method from time series of polar motion excitation functions $\chi(t)$ spanning 1980.0–2001.0 of: (a) the observed COMB2000 polar motion excitation function derived from astrometric and space-geodetic Earth orientation measurements (black curve), (b) the sum of the excitation functions due to atmospheric wind and pressure changes (red curve) where the atmospheric pressure term is that computed assuming the inverted barometer approximation is valid, and (c) the sum of the excitation functions due to atmospheric wind and pressure (inverted barometer) changes as well as oceanic current and bottom pressure changes (blue curve). The retrograde component of polar motion excitation is represented by negative frequencies, the prograde component by positive frequencies.

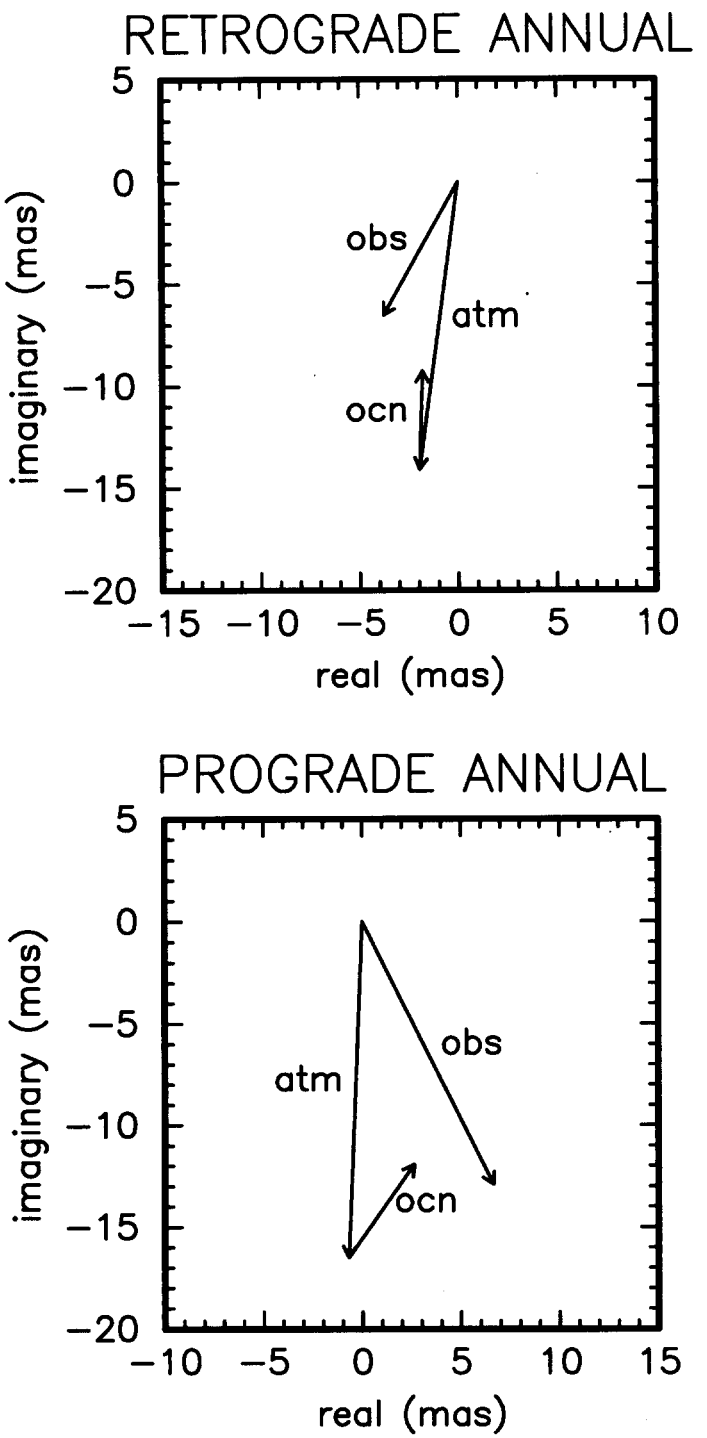

Figure 3. Phasor diagrams of the retrograde and prograde components of the observed (obs), atmospheric (atm), and oceanic (ocn) excitation functions at the annual frequency. The atmospheric results include the effects of both winds and surface pressure where the pressure term was computed assuming that the oceans respond as an inverted barometer to the imposed surface pressure variations; the oceanic results include the effects of both currents and ocean-bottom pressure. The reference date for the phase is January 1.0, 1990.

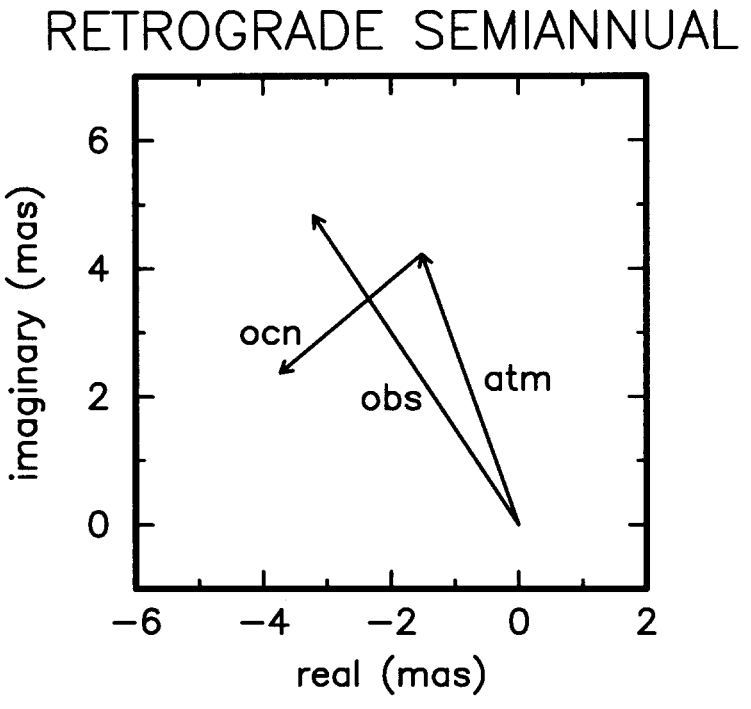

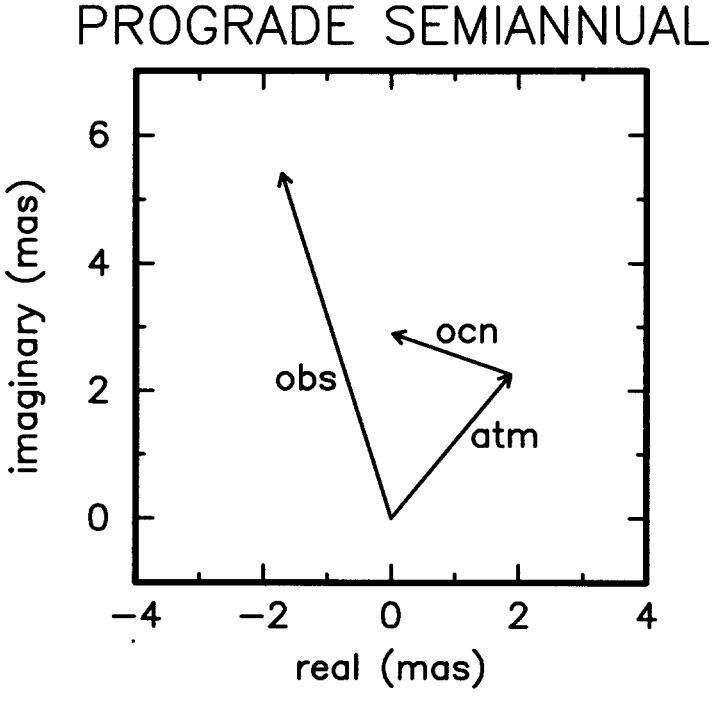

Figure 4. As in Figure 3 but for the excitation of the semiannual wobble.

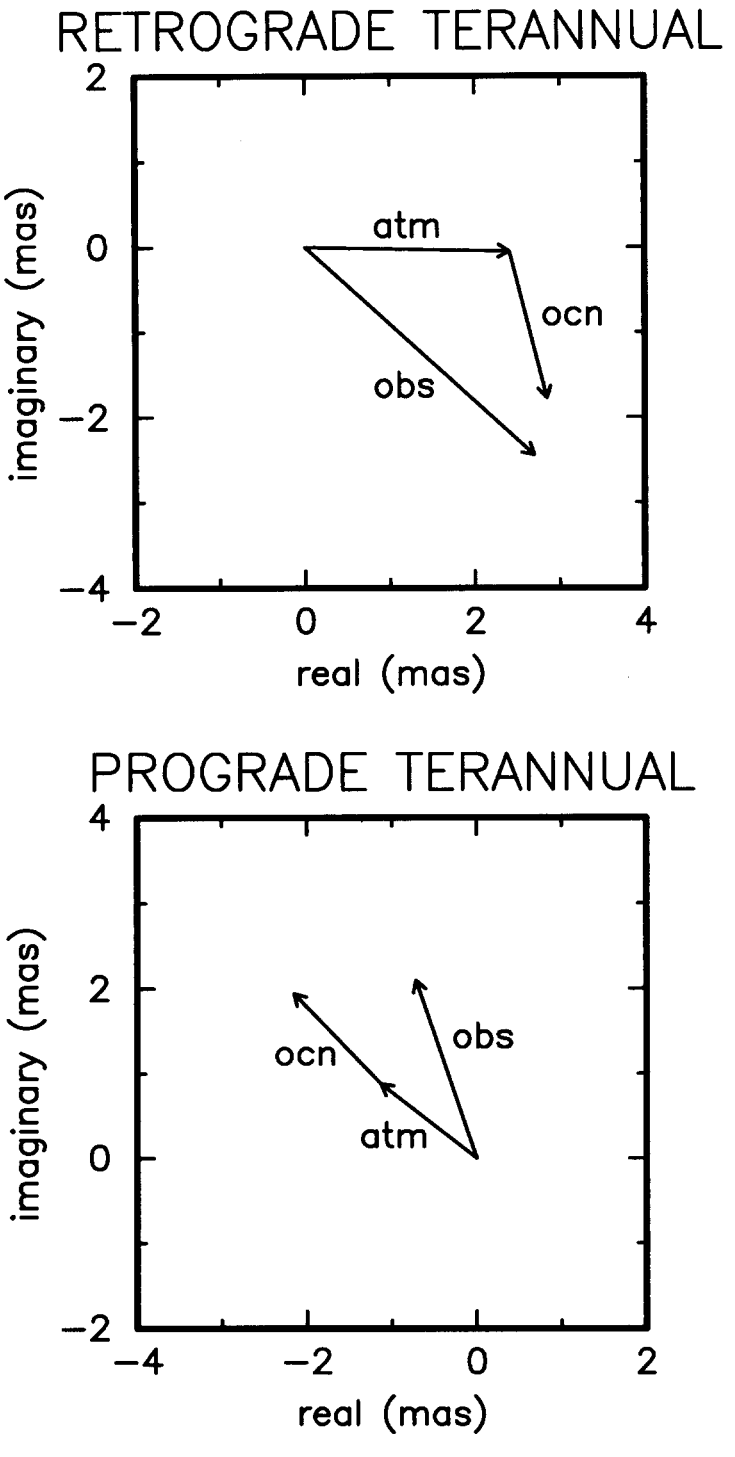

Figure 5. As in Figure 3 but for the excitation of the terannual wobble.

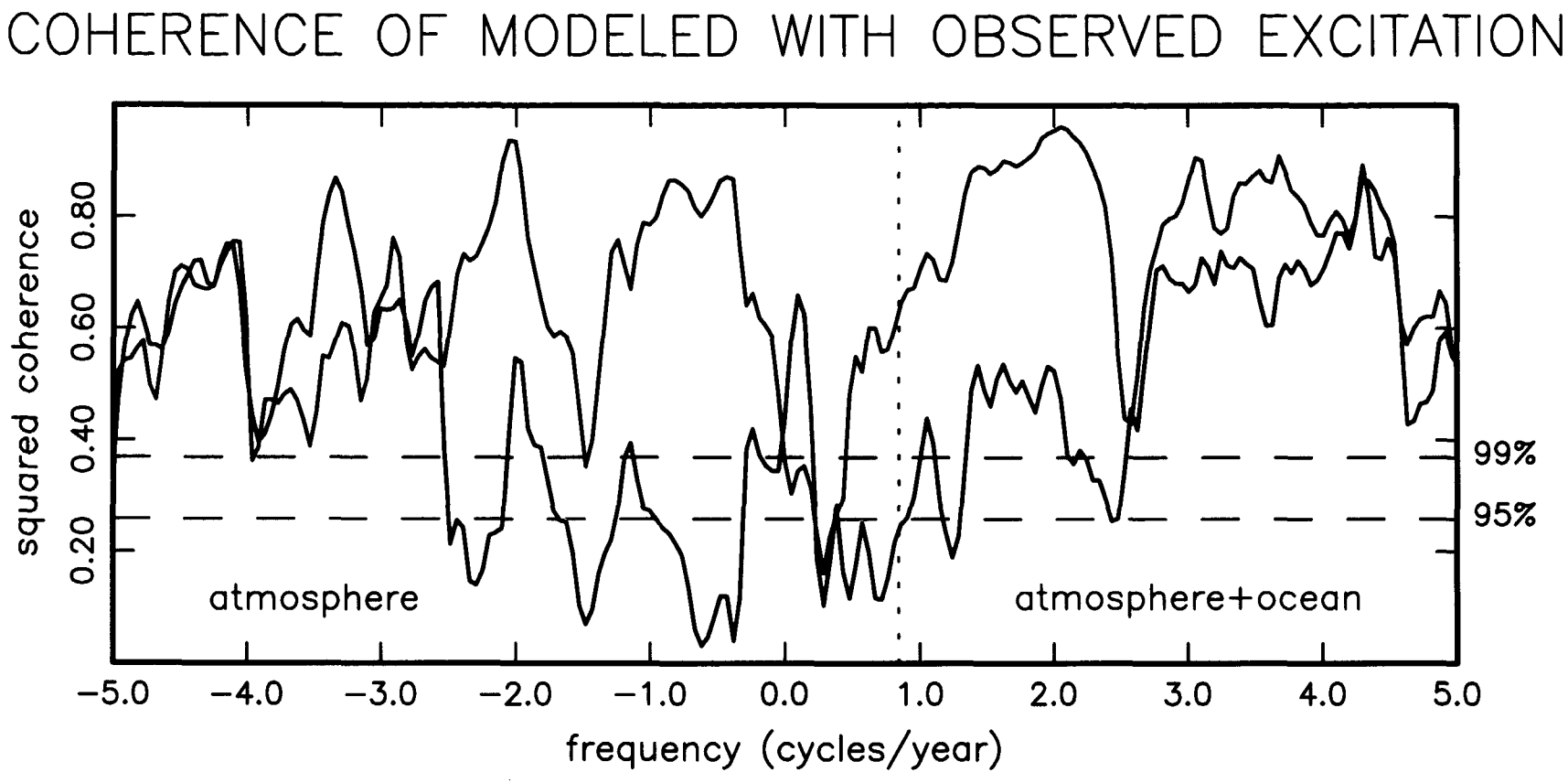

Figure 6. The magnitude of the squared-coherence between the observed polar motion excitation functions spanning 1980.0–2001.0 and the excitation functions due to: (a) the sum of atmospheric wind and pressure changes (red curve) where the pressure term is that computed assuming the inverted barometer approximation for the response of the oceans, and (b) the sum of atmospheric wind and pressure (inverted barometer) and oceanic current and ocean-bottom pressure variations (blue curve). A seasonal signal has been removed from all series prior to coherence estimation by least-squares fitting and removing a mean, a trend, and periodic terms at the annual, semiannual, and terannual frequencies. The vertical dotted line indicates the Chandler frequency of 0.8435 cpy and the horizontal dashed lines indicate the 95% and 99% confidence levels of the magnitude of the squared-coherence.

Table 4. Chandler Band Excitation Power

Excitation process	Power, mas^2
Observed	1.90
Atmospheric	
wind	0.29
pressure (i.b.)	0.65
wind plus pressure (i.b.)	1.03
Oceanic	
currents	0.12
ocean-bottom pressure	0.96
currents plus ocean-bottom pressure	0.66
Atmospheric plus oceanic	
wind plus currents	0.70
i.b. plus ocean-bottom pressure	2.47
Total of all atmospheric plus oceanic	2.22

i.b., inverted barometer; Chandler band is 0.81–0.91 cpy

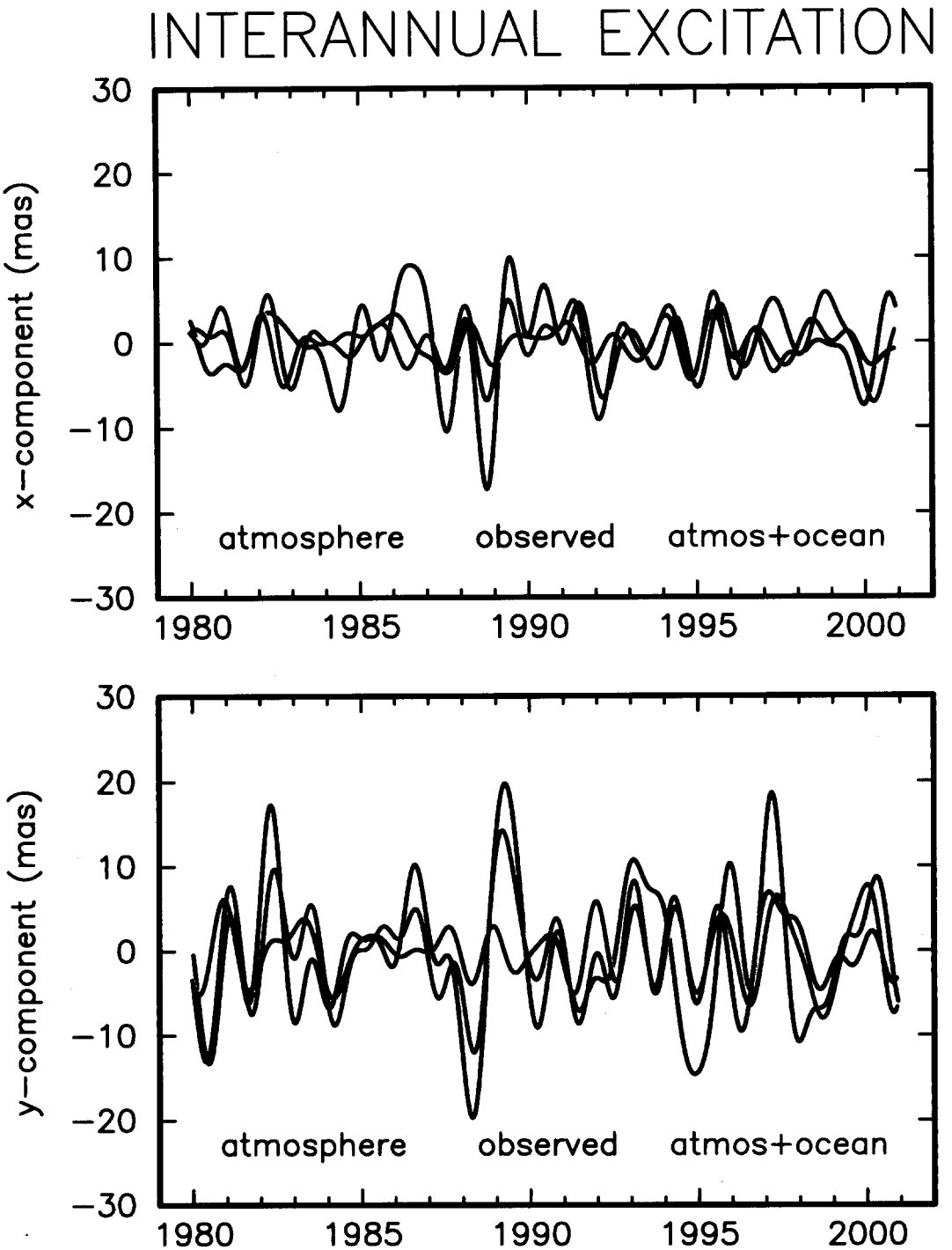

Figure 7. The x- and y-components of the observed (black), the sum of atmospheric wind and pressure (red), and the sum af atmospheric wind and pressure and oceanic currents and ocean-bottom pressure (blue) excitation functions on interannual time scales. Interannual wobbles are defined here to be wobbles having periods between 1 year and 6 years. The atmospheric pressure term is that computed assuming the ocean response to the imposed surface pressure variations is as an inverted barometer.

Table 5. Interannual Wobble Excitation

Excitation process	X	Y	X + *i* Y
% of obs. excitation variance explained by			
atmospheric			
wind	12.1	−6.9	−2.2
pressure (i.b.)	−19.6	4.1	−1.7
wind plus pressure (i.b.)	3.5	6.5	5.8
oceanic			
currents	−9.5	19.4	12.2
ocean-bottom pressure	12.4	36.2	30.3
currents plus bottom pressure	2.8	43.3	33.3
atmospheric plus oceanic			
wind plus currents	−6.2	12.0	7.5
i.b. plus ocean-bottom pressure	−4.7	42.3	30.7
total of all atmospheric plus oceanic	7.4	50.7	40.0
Correlation of observed excitation with			
atmospheric			
wind	0.35	0.05	0.15
pressure (i.b.)	−0.03	0.25	0.18
wind plus pressure (i.b.)	0.26	0.29	0.28
oceanic			
currents	−0.02	0.55	0.48
ocean-bottom pressure	0.36	0.68	0.59
currents plus bottom pressure	0.30	0.67	0.59
atmospheric plus oceanic			
wind plus currents	0.21	0.35	0.37
i.b. plus ocean-bottom pressure	0.26	0.67	0.56
total of all atmospheric plus oceanic	0.39	0.71	0.64

X, *x*-component; Y, *y*-component; %, percentage; obs., observed; i.b., inverted barometer; 99% significance level for correlations is 0.36; interannual frequency band ranges from 1/6 cpy to 1 cpy

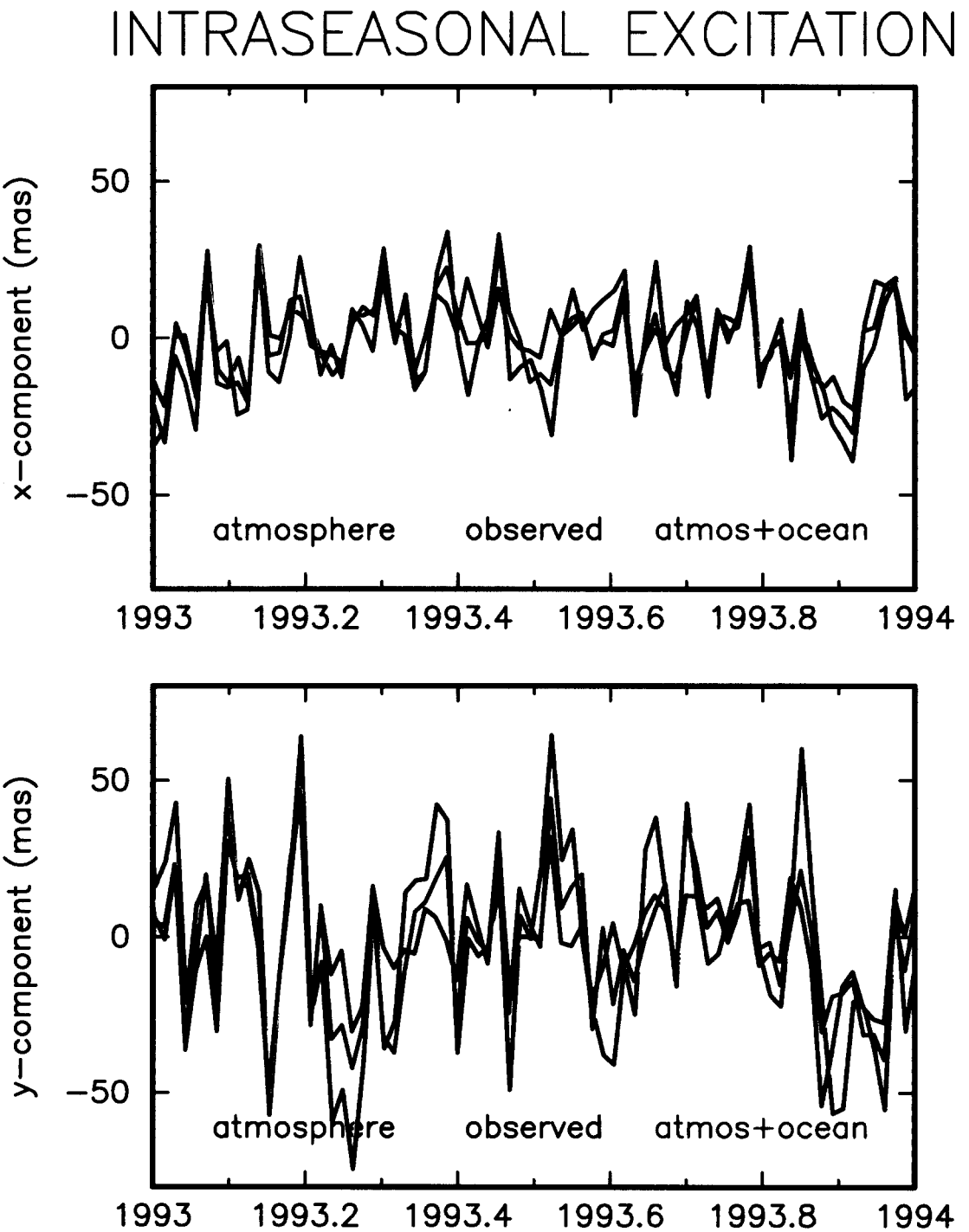

Figure 8. The x- and y-components of the observed (black), the sum of atmospheric wind and pressure (red), and the sum of atmospheric wind and pressure and oceanic currents and ocean-bottom pressure (blue) excitation functions on intraseasonal time scales during 1993. Intraseasonal wobbles are defined here to be wobbles having periods between 5 days and 1 year. The atmospheric pressure term is that computed assuming the ocean response to the imposed surface pressure variations is as an inverted barometer.

Table 6. Intraseasonal Wobble Excitation

Excitation process	X	Y	X + *i* Y
% of obs. excitation variance explained by			
atmospheric			
wind	18.9	19.6	19.4
pressure (i.b.)	21.3	38.2	33.5
wind plus pressure (i.b.)	36.5	47.8	44.6
oceanic			
currents	3.1	10.4	8.4
ocean-bottom pressure	17.8	14.6	15.5
currents plus bottom pressure	16.6	19.4	18.6
atmospheric plus oceanic			
wind plus currents	20.9	28.6	26.5
i.b. plus ocean-bottom pressure	42.2	53.6	50.4
total of all atmospheric plus oceanic	61.3	66.9	65.3
Correlation of observed excitation with			
atmospheric			
wind	0.44	0.52	0.49
pressure (i.b.)	0.47	0.64	0.59
wind plus pressure (i.b.)	0.61	0.69	0.67
oceanic			
currents	0.20	0.40	0.31
ocean-bottom pressure	0.43	0.39	0.41
currents plus bottom pressure	0.42	0.44	0.44
atmospheric plus oceanic			
wind plus currents	0.46	0.61	0.54
i.b. plus ocean-bottom pressure	0.65	0.76	0.73
total of all atmospheric plus oceanic	0.78	0.82	0.81

X, *x*-component; Y, *y*-component; %, percentage; obs., observed; i.b., inverted barometer; 99% significance level for correlations is 0.08; intraseasonal wobbles considered here have periods ranging between 5 days and 1 year

ACKNOWLEDGMENTS

- The work of RSG described in this presentation was performed at the Jet Propulsion Laboratory, California Institute of Technology, under contract with the National Aeronautics and Space Administration.